

Relics of the Cosmological QCD Phase Transition

Abhijit Bhattacharyya^a, Jan-e Alam^{a1}, Sourav Sarkar^a, Pradip Roy^a,
Bikash Sinha^{a,b}, Sibaji Raha^c and Pijushpani Bhattacharjee^{d,e}

a) Variable Energy Cyclotron Centre, 1/AF Bidhan Nagar, Calcutta 700 064, India

b) Saha Institute of Nuclear Physics, 1/AF Bidhan Nagar, Calcutta 700 064, India

c) Department of Physics, Bose Institute, 93/1, A.P.C. Road, Calcutta 700 009, India

*d) Laboratory for High Energy Astrophysics, NASA/Goddard Space Flight Centre,
Code 661 Greenbelt, MD 20771, USA*

e) Indian Institute of Astrophysics, Bangalore - 560 034 India

Abstract

The abundance and size distribution of quark nuggets (QN), formed a few microseconds after the big bang due to first order QCD phase transition in the early universe, has been estimated. It appears that stable QNs could be a viable candidate for cosmological dark matter. The evolution of baryon inhomogeneity due to evaporated (unstable) QNs are also examined.

PACS : 98.80.Cq, 12.38.Mh, 95.35.+d

1 Introduction

As per the standard model, the universe, after a few micro seconds of the big bang, underwent a phase transition from quarks and gluons to hadrons. There are well organised efforts to mimic such a phase transition in the laboratory through heavy ion collisions at ultra-relativistic energies [1]. Although there are similarities between the two scenarios, the relatively long time scales in the early universe phase transition may indeed be more conducive to a reliable thermodynamic description. In the absence of any consensus on the order of QCD phase transition for two light and one medium-heavy quarks from lattice calculations [2] in the present work we assume an underlying picture of a first order phase transition [3] from quarks and gluons to hadrons. The central question we would like to address is what plausible

¹Present Address: Physics Department, Kyoto University, Kyoto 606-8502, Japan

remnants may have survived since that primordial epoch. Crawford and Schramm [4] and Van Hove [5] argued that fluctuations in the horizon scale, triggered by the phase transition, may lead to the formation of primordial black holes, which could be as large as M_{\odot} , the solar mass. Schramm [6] has recently suggested that these black holes could even be the candidates for the Massive Compact Halo Objects (MACHO's) [7, 8], which had of late been discovered in the halo of the Milky way, in the direction of the Large Magellanic Cloud (LMC) using the gravitational lensing techniques. On the other hand, a first order QCD phase transition scenario involving bubble nucleation at a critical temperature $T_c \sim 100 - 200$ MeV could lead to the formation of quark nuggets (QN), made of u , d and s quarks at a density somewhat larger than normal nuclear matter density. If these primordial QN's indeed survive till the present epoch, they could be a possible candidate for the baryonic component of the dark matter [3]. Such a possibility would be aesthetically rather pleasing, as it would not require invoking any exotic physics nor would the success of the primordial (Big Bang) nucleosynthesis scenario be materially affected [9, 10, 11, 12].

The central question in this context is, thus, whether the primordial QN's can be stable on a cosmological time scale. The first study on this issue was addressed by Alcock and Farhi [13] who argued that neutrons could be liberated and emitted from a QN at temperature $T \geq I_N$, where I_N (~ 20 -80 MeV) is the neutron "binding energy" *i.e.* the difference between energy per baryon in strange matter at zero temperature and the mass of the nucleon. They calculated the rate of baryon evaporation from QNs by using detailed balance between the two processes of neutron absorption and emission in a system consisting of QNs (of all possible baryon numbers) and neutrons. They also assumed a geometric cross section for the neutron absorption by the QNs and complete transparency of the nugget surface to neutrons. This gave the result that QNs even with the largest allowed initial baryon number (*i.e.* the total baryon number $N_{B,hor} \approx 10^{49}(100\text{MeV}/T)^3$ contained in a horizon-size volume of the universe, at the time of formation of the nugget, T being the temperature of the universe at that time) were unstable with respect to baryon evaporation. These results apparently eliminated the possibility of any QN surviving till the present epoch.

Madsen et al [14] then pointed out that, since evaporation was a surface process,

emission of neutrons (proton emission was suppressed due to the Coulomb barrier) made the surface layer deficient in u and d quarks, although relatively enriched in s quarks. The rate of conversion of s quarks back to u and d quarks as well as convection of u and d quarks from the core of the nugget to the surface were both too slow to establish flavor chemical equilibrium between u , d and s quarks on the surface layer. As a result of this deficiency of u and d quarks in the surface layer, further nucleon evaporation was suppressed. Madsen et al found that QNs with initial baryon number $N_B \geq 10^{46}$ could well be stable against baryon evaporation.

QNs at temperatures above a few MeV could also be subject to the process of "boiling" [15], *i.e.*, spontaneous nucleation of hadronic bubbles in the bulk of the nugget and consequent conversion of the nugget into nucleons. Madsen and Olesen [16] however, showed that although boiling is thermodynamically allowed, the time scale for bubble nucleation inside QNs is too long compared to the time scale of surface evaporation for reasonable values of the parameters used.

All of the above studies used thermodynamic and binding energy arguments to calculate the baryon evaporation rate; the microscopic dynamics determining the probability of baryon formation and emission had been neglected. Clearly, for a realistic description of the process a dynamical model of baryon emission from QNs was needed.

Earlier, Bhattacharjee *et al* [17] used the chromoelectric flux tube model (inspired by QCD) to demonstrate that the QN's would survive against baryon evaporation, if the baryon number of the quark matter inside the nugget was larger than 10^{42} . For reasons explained in ref. [17], this estimate is rather conservative. Sumiyoshi and Kajino [18] estimated within a similar approach that a QN with an initial baryon number $\sim 10^{39}$ would survive against baryon evaporation.

It may also be mentioned in this context that Madsen and Riisager [12] had calculated the minimum size of the QNs from the constraint imposed by the primordial He abundance. The authors showed that the minimum radius of the QNs should be more than $\sim 10^{-6}$ cm, otherwise the absorption of neutrons by the QNs will upset the neutron to proton ratio in the universe, resulting in a helium abundance in complete disagreement with the experimental results.

In spite of these efforts, not much attention has been paid towards the issues

of formation and size-distribution of the surviving quark nuggets in the universe. The size-distribution and abundance of the QNs is very important in the context of their candidature as dark matter. The calculation of a lower cut-off in size, if any, would tell us what can be the minimum size and the baryon number content of a QN that we should look for. On the other hand, the distribution function also indicates the most probable size of the QNs. Such studies in the framework of the GUT (Grand Unified Theory) phase transition and the associated "Trapped False Vacuum Domains" (TFVD) have been done earlier [19]. The basic contention of this paper is to carry out these studies for the QCD phase transition in the early universe. We also study the evolution of baryon inhomogeneity created by evaporating QNs, with baryon number lower than the survivability window, as mentioned above, due to the conduction of heat by neutrinos, and consequently the dissipation of the baryon inhomogeneities.

We organise the paper as follows. In the next section we evaluate the size-distribution of the QNs. The results for different nucleation rates have been discussed. Section 3 contains the evolution of baryon inhomogeneity which originated due to the unstable QNs. In section 4 we conclude.

2 The size-distribution of quark nuggets

The evolution of the universe during the QCD phase transition is governed by Einstein's equations,

$$\left(\frac{\dot{R}}{R}\right)^2 = \frac{8\pi\rho}{3m_{pl}^2}; \quad \frac{d(\rho R^3)}{dt} + P\frac{dR^3}{dt} = 0 \quad (1)$$

where ρ is the energy density, P the pressure and m_{pl} the Planck mass. In the above equation, R is the cosmological scale factor in the Robertson-Walker space time and is defined by the relation

$$\begin{aligned} ds^2 &= -dt^2 + R^2 dx^2 = R^2(-d\xi^2 + dx^2) \\ dx^2 &= dX^2 + X^2(\sin^2\theta d\phi^2 + d\theta^2) \end{aligned} \quad (2)$$

where X is the co-ordinate radius *i.e.* the radius in the unit of the cosmological scale factor $R(t)$.

It is well known that in a first order phase transition, the quark and the hadron phases co-exist in a mixed phase at the critical temperature of transition. Around the critical temperature, the universe consists of leptons, photons and the massless quarks, anti-quarks and gluons, described in our case by the MIT bag model with an effective degeneracy $g_q(\sim 51.25)$. The hadronic phase contains relativistic π -mesons, photons and leptons with a small baryon content ($\rho_B/\rho_\gamma \sim 10^{-10}$) and is described by an equation of state corresponding to massless particles with an effective degeneracy $g_h = 17.25$. The energy densities and the pressures of hadronic and quark matter are given by

$$\begin{aligned}\rho_h &= \frac{\pi^2 g_h}{30} T^4; & \rho_q &= \frac{\pi^2 g_q}{30} T^4 + B \\ P_h &= \frac{\pi^2 g_h}{90} T^4; & P_q &= \frac{\pi^2 g_q}{90} T^4 - B\end{aligned}\quad (3)$$

where B is the bag constant.

The evolution of the scale factor in the mixed phase is given by (see also [20]),

$$R(t)/R(t_i) = \left[\cos \left(\arctan \sqrt{3r} - \sqrt{\frac{3}{r-1}} (t - t_i)/t_c \right) \right]^{2/3} / \left[\cos \left(\arctan \sqrt{3r} \right) \right]^{2/3}\quad (4)$$

In the process we also get the volume fraction of the quark matter $f(t)$ in the mixed phase as

$$f(t) = \frac{1}{3(r-1)} \left[\tan \left\{ \arctan \sqrt{3r} - \sqrt{\frac{3}{r-1}} \frac{t - t_i}{t_c} \right\} \right]^2 - \frac{1}{r-1}\quad (5)$$

where $r \equiv \rho_q/\rho_h$, $t_c = \sqrt{3m_{pl}^2/8\pi B}$ is the characteristic time scale for the QCD phase transition in the early universe and t_i is the time when phase transition starts. (The definition of r and hence the expressions of $R(t)$ and $f(t)$ here are somewhat different from that in ref. [20]). The characteristic time scale depends on the bag constant and hence on the critical temperature of the quark-hadron phase transition (T_c). In fact $t_c = 144\mu s$ for $T_c = 100 MeV$ and $t_c = 64\mu s$ for $T_c = 150 MeV$.

In the coexisting phase, the temperature of the universe remains constant at T_c , the cooling due to expansion being compensated by the liberation of the latent heat. In the usual picture of bubble nucleation in a first order phase transition scenario hadronic matter starts appearing as individual bubbles. With the progress of time,

more and more hadronic bubbles form, coalesce and eventually percolate to form an infinite network of hadronic matter which traps the quark matter phase into finite domains. The time when the percolation takes place is usually referred to as the percolation time t_p , determined by a critical volume fraction f_c , ($f_c \equiv f(t_p)$) of the quark phase.

In an ideal first order phase transition, the fraction of the high temperature phase decreases from the critical value f_c , as these domains shrink. For the QCD phase transition, however, these domains could become QN's and as such, we may assume that the lifetime of the mixed phase $t_f \sim t_p$.

As mentioned above, just after percolation one can have pockets of quark matter trapped as bubbles in the ambient hadronic matter. The probability that a spherical region of co-ordinate radius X at time t_p with nucleation rate $I(t)$ lies completely within the quark matter domain is given by [19],

$$P(X, t_p) = \exp \left[-\frac{4\pi}{3} \int_{t_i}^{t_p} dt I(t) R^3(t) (X + X(t_p, t))^3 \right] \quad (6)$$

where $X(t_p; t)$ is the coordinate radius of a bubble, at time t_p , which was nucleated at time t .

For convenience, let us now define a new set of variables $z = XR(t_i)/vt_c$, $x = t/t_c$ and $r(x) = R(x)/R(x_i)$; where v is the radial growth velocity of the nucleating bubbles. Then

$$P(z, x_p) = \exp \left[-\frac{4\pi}{3} v^3 t_c^4 \int_{x_i}^{x_p} dx I(x) (zr(x) + y(x_p, x))^3 \right] \quad (7)$$

where

$$y(x, x') = \int_{x'}^x r(x'')/r(x'') dx'' \quad (8)$$

So the fraction of quark matter present at time t_p is

$$f_c = P(0, x_p) = \exp \left[-\frac{4\pi}{3} v^3 t_c^4 \int_{x_i}^{x_p} dx I(x) y^3(x_p, x) \right] \quad (9)$$

Let us now look at the size-distribution of the Trapped Quark Matter Domain (TQMD). In order to do so we will follow the procedure of ref. [19]. The difference of our work from that of Kodama *et al.* is that we have considered exactly spherical nuggets whereas they have included a deformation factor. It should however be

noted that the deformation factor, as found by Kodama *et al*, is small. Moreover, due to the presence of non-zero surface tension in case of QCD phase transition the bubbles are likely to be spherical. Even more importantly, we focus our attention to the percolation time t_p when the hadronic matter forms the ambient background. All these considerations allow us to consider the false vacuum domains (the quark phase) as being spherical in shape. Following Ref. [19] let us assume that $F(X; t)dX$ is the number of TQMDs per unit volume within the size $\{X, X + dX\}$ at time t . Then $P(X, t)$ can be thought to be the probability that a QN of coordinate radius X at a fixed position is contained in a TQMD. Now a TQMD of size η can contain such a sphere of size X only when the center of TQMD lies within the coordinate radius $\eta - X$ from the center of the sphere. If α is the minimum size of a TQMD *i.e.* $F(X, t)$ vanishes for $X < \alpha$ then one can write

$$P(X; t) = \int_{\alpha+X}^{\infty} \frac{4\pi}{3} (\eta - X)^3 F(\eta; t) d\eta \quad (10)$$

The distribution function vanishes for $X < \alpha$. One can now solve the above equation using Laplace transformation to obtain $F(X)$ (see appendix).

The result, in terms of z , is

$$\begin{aligned} F(z) &= \frac{3\theta(z - \alpha)R(t_i)^4}{4\pi\alpha^3v^4t_c^4} \left[-P'(X - \alpha) - \frac{3P(X - \alpha)}{\alpha} \right. \\ &+ \left. \frac{1}{\alpha^2} \int_0^{\infty} d\eta P(\eta + X - \alpha) \left\{ \lambda e^{(-\lambda\eta/\alpha)} + \omega e^{(-\omega\eta/\alpha)} + \bar{\omega} e^{(-\omega\eta/\alpha)} \right\} \right] \\ &= \frac{R(t_i)^4}{v^4t_c^4} f(z) \end{aligned} \quad (11)$$

The solution of the equation $F(\alpha) = 0$ gives the minimum size of the quark-nugget α . Now, the number of nuggets per unit volume is given by

$$\begin{aligned} n_Q &= R^{-3}(t_p) \int_{\alpha}^{\infty} F(X) dX \\ &= R^{-3}(t_p) \int_{\alpha}^{\infty} \frac{R^3(t_i)}{v^3t_c^3} f(z) dz \end{aligned} \quad (12)$$

The volume of each quark nugget is given by $\frac{4}{3}\pi(zvt_c)^3$. Since the visible baryon constitutes only ten per cent of the closure density ($\Omega_B = 0.1$ from standard big bang nucleosynthesis), a total of 10^{50} baryons will close the universe baryonically at $T = 100$ MeV. We emphasize at this point that these QNs would not disturb

the standard primordial nucleosynthesis results to any considerable extent, as they would not participate in usual nuclear reactions. Therefore, if we assume that the total baryon content of the dark matter is carried by the quark nuggets, then,

$$N_B = 10^{50}(100/T(\text{MeV}))^3 = V_H \frac{4\pi R^3(t_i)}{3R^3(t_p)} \rho_B \int_{\alpha}^{\infty} f(z) z^3 dz \quad (13)$$

where V_H is the horizon volume and ρ_B is the baryon density inside each nugget. We now solve the above equations self-consistently to obtain α , t_p and f_c . These values are then used to study the size-distribution of the quark nuggets.

To calculate the size and distribution of QNs we need to know the rate of nucleation during the phase transition process. Many authors [23, 24] have proposed various nucleation rates for the QCD phase transition. In the absence of a consensus as to which rate is preferable to others, we look at several of them. We begin with the rate proposed by Cottingham *et.al.* [23] which is based on the Lee-Wick model of effective QCD. They calculated the Lee-Wick potential at finite temperature to obtain the following nucleation rate

$$I(t) = T^4 \left(\frac{S}{2\pi T} \right)^{3/2} \exp(-S/T) \quad (14)$$

with

$$\begin{aligned} S &= \frac{2\pi}{3} \left(\frac{m\sigma_0^2}{3} \right)^3 \frac{1}{P^2} \\ P &= \frac{7\pi^2}{30} (T_c^4 - T^4) \end{aligned} \quad (15)$$

where $\sigma_0 = 100\text{MeV}$ and $m = 939\text{MeV}$.

Csernai and Kapusta [24] proposed a nucleation rate which is of the form

$$I(t) = r_T \exp \left[-\Delta / (1 - t/t_c)^2 \right] \quad (16)$$

with

$$\Delta = \frac{16\pi\sigma^3}{48B^2T_c} \quad (17)$$

where σ is the surface tension and r_T is a temperature dependent constant. They have calculated the pre-exponential factor r_T from an effective field theory of QCD. This nucleation rate is the same as the general form proposed by Landau and Lifshitz [25], apart from the pre-exponential factor.

σ (MeV/fm ⁻²)	T_c (MeV)	minimum radius (meter)	N_{QN}
Cottingham <i>et. al.</i>	100	1.66	7420
	150	0.083	1.7×10^7
10 Csernai <i>et. al.</i>	100	0.117	2.1×10^7
	150	0.0096	3.8×10^{10}
50 Csernai <i>et. al.</i>	100	1.25	1.7×10^4
	150	0.0882	1.4×10^7

Table 1: Different values of minimum radius and N_B for the different nucleation rates.

Let us discuss the results obtained so far. In table I we have shown the dependence of the minimum radius of a quark nugget and the number of QNs within the horizon just after the QCD phase transition on the value of T_c for different nucleation rates. For the nucleation rate proposed by Csernai and Kapusta, we have varied the surface tension from $\sigma = 10 - 50 MeV fm^{-2}$. We have found that the minimum radius varies from 9.6×10^{-3} meter to 1.66 meter.

In fig. 1 we have plotted the distribution of QN, $f(\bar{n}_B)$, as a function of \bar{n}_B using the nucleation rate proposed by Cottingham *et.al.*, for different values of T_c , where \bar{n}_B is the baryon number content of a single QN. We see that for $T_c = 100 MeV$ distribution of QN peaks at baryon number $\sim 7 \times 10^{45}$ and there is almost no QN with baryon number larger than 10^{47} . For $T_c = 150 MeV$ these values are 10^{42} and 10^{43} respectively. In figs. 2-3, similar results have been shown for nucleation rate proposed by Csernai and Kapusta, for $\sigma = 10$ and $50 MeV fm^{-2}$, respectively. We see that for a fixed T_c , the minimum radius increases with increase in σ . Figure 3 shows that the maximum number of nuggets are around a baryon number of $\sim 2.5 \times 10^{42}$ at $T_c = 100 MeV$ whereas the number of nuggets goes to zero after 4×10^{43} . Similar results for $T_c = 150 MeV$ are also shown in the figures. We should mention at this stage that the lower cutoffs that we have obtained here are certainly allowed by the study of Madsen *et.al.* [12] within the reasonable set of parameters.

The question which arises next is whether these nuggets will survive till the present epoch. Earlier studies [17] have shown that the nuggets having baryon number less than 10^{42} will not survive till the present epoch. This suggests that all the cases considered here for $T_c = 100 MeV$ will give stable nuggets. However, from figure 1 and 3, it can be seen that, for $T_c = 150 MeV$, some of the nuggets will not survive. Fig. 2. suggests that for $\sigma = 10 MeV fm^{-2}$, none of the nuggets will survive when $T_c = 150 MeV$. Given the present state of the art, there is no way to choose any one of the possibilities as the preferred one. We should therefore consider the situation that while some nuggets may indeed be stable and constitute cold dark matter, some smaller nuggets may evaporate, creating sizeable baryon inhomogeneities. In the next section we will study the evolution of these inhomogeneities with time/temperature.

3 Evolution of baryon inhomogeneities due to evaporated quark nuggets

Our aim in this section is to study the implications of those QNs that do evaporate away, *assuming*, of course, that they were formed in the early universe. When a QN dissociates into nucleons, the latter initially form a clump with high baryon overdensity relative to the density of baryons in the ambient universe. The baryon density in the clump then gradually decreases as various physical processes tend to ‘flatten’ the clump. We study the evolution of the highly non-linear baryonic inhomogeneities represented by these high density clumps due to dissociated QNs created after the epoch of quark-hadron phase transition at $T \sim 100\text{MeV}$, T being the temperature of the universe.

The evolution of large, non-linear baryon inhomogeneities in the early universe has been studied in detail recently, especially in the context of possible creation through electroweak baryogenesis process [26, 27, 28] of large baryon inhomogeneities during the epoch of a possible first-order electroweak symmetry-breaking phase transition at $T \sim 100\text{GeV}$. The single most dominant physical process that determines the evolution of large baryon inhomogeneities in the early universe before the epoch of neutrino decoupling (at $T \sim 1\text{MeV}$) is the so-called “neutrino inflation”. Any large baryonic clump in pressure equilibrium with the ambient universe would have a slightly lower temperature inside the clump relative to the temperature of the ambient surroundings, due to the excess pressure contributed by the excess baryons inside the clump. As a result, heat would be conducted into the clump from the ambient medium. The particles most efficient in conducting heat into the clump are the neutrinos which have, by far, the largest mean free path (MFP) amongst all the relevant elementary particles. As neutrinos cross the clump they deposit energy into the clump thereby heating up the clump. The clump then expands in order to achieve pressure equilibrium under this changed circumstance, and so the baryon density within the clump decreases as the clump expands. This process of expansion (“inflation”) of the clump due to neutrino heat conduction continues until the neutrinos decouple at around $T \sim 1\text{MeV}$. For any given size of a clump, the time scale on which a clump achieves pressure equilibrium with the

surroundings is essentially the hydrodynamic expansion time scale or the time taken by sound to traverse the clump, which can be shown to be smaller than the heat transport time scale for neutrinos. It is, therefore, a good approximation to treat the evolution of the clump as going through a succession of pressure equilibrium stages with decreasing density inside the clump. After neutrino decoupling the evolution of the clump is determined mainly by the process of baryons slowly diffusing out of the high-density clump to the ambient medium.

In this section, we study the evolution of the baryonic clumps created by evaporated QNs under neutrino inflation. It is to be mentioned here that the linear relationship, assumed in ref.[26], between the baryon overdensity within a clump and the fractional temperature difference of the clump relative to the ambient temperature, turns out to be invalid in our case of extremely large initial baryon overdensity created by the evaporated QNs, as we discuss below. As a consequence, we need to numerically solve the full non-linear pressure equilibrium equation for a clump in order to obtain the relationship between those quantities. Furthermore, the initial baryon overdensity within the clump in our case can be so large (e.g. $\sim 10^{12}$)[21] that baryon-to-entropy ratio within the clump could be initially greater than unity in which case the dominant contribution to the MFP of neutrinos would come initially from neutrino-nucleon scattering rather than from neutrino-lepton scattering assumed in ref.[26]. The above two considerations make a straightforward application of the results of ref.[26] invalid in our case of large baryonic inhomogeneities due to evaporating QNs; hence the need to do an *ab initio* calculation for inhomogeneities with initial overdensity significantly larger than those studied in ref.[26]. In this respect, we believe the calculations in this paper, although done in the specific context of inhomogeneities due to quark nuggets, have much wider validity and application. We would like to mention at this stage that we are interested to study only the neutrino inflation process which will be operative till $T = 1MeV$. So we restrict our calculation upto that temperature. Also, the only difference from the work of ref. [26] is that we have solved the full non-linear pressure equation.

The pressure equilibrium equation for a baryonic clump with baryon number density $\rho_B^* \equiv \delta_N \rho_B$ and temperature $T^* \equiv T(1 - \delta T)$ in the background universe at

temperature T and baryon number density ρ_B can be written as

$$\rho_B^* T^* + \frac{1}{3}g_{eff}(T^*)aT^{*4} = \rho_B T + \frac{1}{3}g_{eff}(T)aT^4 \quad (18)$$

where $g_{eff}(T)$ is the effective number of relativistic degrees of freedom in the universe at temperature T contributing to the energy density and pressure, and $a = \pi^2/30$. The baryons within the clump as well as outside are assumed to be ideal gases of non-relativistic particles with pressures $\rho_B^* T^*$ and $\rho_B T$, respectively. Assuming $\delta_N \geq 1$, $\delta T \leq 1$, and $g_{eff}(T^*) \approx g_{eff}(T)$, we get from eq.(18),

$$\delta T \simeq \frac{\eta \delta_N}{1 + \eta \delta_N} \quad (19)$$

where $\eta = \rho_B/s$, s being the entropy density. The baryon-to-entropy ratio η in the universe is essentially constant for the temperature range of our interest, $s \approx 2.6 \times 10^8 \Omega_B^{-1} h^{-2}$, where Ω_B is the baryonic mass density in the universe in units of the closure density, and $h = H_0/(100 km, sec^{-1}, mpc^{-1})$, H_0 being the present value of the Hubble constant.

Eq.(19) shows that if the baryon overdensity δ_N in the clump satisfies the condition $\eta \delta_N \ll 1$, then $\delta T \simeq \eta \delta_N$, i.e., δT is linearly proportional to δ_N [26]. On the other hand, for overdensities satisfying $\eta \delta_N \gg 1$, Eq.(19) gives $\delta T \sim 1$, which is inconsistent with the assumption $\delta T \ll 1$ under which Eq.(19) is derived. Clearly, then, for sufficiently large overdensities for which $\delta_N \geq \eta^{-1}$, the assumption $\delta T \ll 1$ is not valid, and so we need to solve the full non-linear pressure equilibrium equation, Eq.(18), to obtain the relationship between δT and δ_N . This is the essential difference between our work and that of ref.[26]. The result is demonstrated in figure 4.

Now, for a given overdensity δ_N of the clump at some time t when the temperature of the universe is T , the rate of energy deposited into the clump by neutrinos depends upon whether the size L ($= 2R$, R being the radius) of the clump (assumed spherical) is larger or smaller than the MFP (λ_ν), of neutrinos through the clump at that time. For $\lambda_\nu \leq L$ the clump will not inflate by any significant amount because the energy deposition by ambient neutrinos will occur mainly in a thin surface layer of the clump leaving the bulk of the clump unaffected. Indeed in this case the heating of the clump will be governed by slow diffusion [27] of neutrinos inside the

clump. However, λ_ν in the early universe increases rapidly as T decreases, typically, $\lambda_\nu \propto T^{-5}$. This means that a clump of any given size L will quickly come within the “neutrino horizon”, such that λ_ν becomes larger than L before any significant neutrino inflation of the clump takes place. Indeed, most of the neutrino inflation of the clump will take place when $L \sim \lambda_\nu$ and $L \geq \lambda_\nu$. The evolution of δ_N with time (temperature) is governed by the following differential equations [26, 29]

$$\frac{d\delta_N}{dt} = -\frac{4}{R} \frac{\rho_\nu}{\rho} \delta T \delta_N \quad (20)$$

for $L \sim \lambda_\nu$,

$$\frac{d\delta_N}{dt} = -\frac{3}{4} \frac{1}{\lambda_\nu} \frac{\rho_\nu}{\rho} \delta T \delta_N \quad (21)$$

for $L > \lambda_\nu$.

The typical values of the overdensity δ_N and size L of those overdensities expected from QN evaporation, are calculated by Iso et al [21]. The values of δ_N could be as large as 10^{12} and $R \sim 10$ cm. Since nothing is known about the initial overdensity δ_N and the length scale L , we study the evolution of the baryon overdensities for various initial values of δ_N and L by solving equation (20) and (21). In figure 4 we have shown the importance of considering the non-linear term. It can be seen from the figure that at high $\delta T/T$ the linear relation breaks down quite substantially. The nuggets which will not be stable against evaporation will form highly dense baryonic lumps. We have studied the evolution of these lumps with time. Neutrinos play an important role in the evolution of these lumps up to 1 MeV. The results are shown in fig. 5. Lumps with initial overdensity $\leq 10^8$ is not affected by the neutrino conduction. The final values of the overdensity is smaller for higher initial temperature.

From the above discussion and fig. 5 it is clear that some overdensity is left out after the neutrino inflation which is of the order of 10^7 . This overdensity, as it looks, is a sizeable amount. The baryon diffusion starts dominating after the neutrinos fall out of equilibrium ($T \sim 1\text{MeV}$). From $T = 1\text{MeV}$ to the beginning of the nucleosynthesis *i.e.* $T = 0.1\text{MeV}$ baryon diffusion is the most dominant process as far as the dissipation of the overdensities are concerned. If the baryon diffusion lengths are larger than the typical size of the inhomogeneities then the

overdensities will be washed out due to this process. As a result these objects will not alter the standard big bang nucleosynthesis scenario. This has been shown for the baryon inhomogeneity created at the Electro-Weak scale by Brandenberger *et. al.* [30]. These findings once again supports the existence of nuggets. If the evaporating nuggets would have left very high asymmetries in the universe then the observed He^4 abundance, which is thought be very well determined, would have been violated, a scenario not very comfortable with the survival of quark nuggets.

4 Conclusion

In this work we have estimated the abundance of quark nuggets in various nucleation scenarios with different values of critical temperature and surface tension of the bubble. We have found that within a reasonable set of parameters QNs may be a possible candidate for cosmological dark matter. The evolution of baryon inhomogeneities, formed due to the unstable QNs have also been studied.

5 Appendix

In this appendix we follow Ref. [19] to solve the following integral equation,

$$P(X; t) = \int_{\alpha+X}^{\infty} \frac{4\pi}{3} (\eta - X)^3 F(\eta; t) d\eta \quad (22)$$

Differentiating the above equation for four times we get

$$\frac{3}{4\pi} P^{(4)}(X) = -D(\alpha\partial_X) F(X) \quad (23)$$

where

$$D(\alpha\partial_X) = \alpha^3 \frac{\partial^3}{\partial X^3} - 3\alpha^2 \frac{\partial^2}{\partial X^2} - 6\alpha \frac{\partial}{\partial X} - 6 \quad (24)$$

Let

$$\mathcal{L}(F(X)) = \bar{F}(p) = \int_0^{\infty} F(X) e^{-pX} dp \quad (25)$$

where $\mathcal{L}(A)$ is the Laplace transform of A . Now using the Laplace transformations of the derivatives we have

$$\frac{3}{4\pi} P^{(4)}(X) = D(\alpha p) \bar{F}(p) e^{-\alpha p} \quad (26)$$

where we have neglected an arbitrary constant. Now,

$$\begin{aligned}
F(X) &= \frac{3}{4\pi} \frac{1}{2\pi i} \int_{c-i\infty}^{c+i\infty} \frac{P^{(4)}(p)}{D(\alpha p)} e^{p(X-\alpha)} dp \\
&= \frac{3}{4\pi} \int_0^\infty d\eta P^{(4)}(\eta) \frac{1}{2\pi i} \int_{c-i\infty}^{c+i\infty} \frac{e^{p(X-\alpha-\eta)}}{D(\alpha p)} dp \\
&\times \left[-P^{(1)}(X-\alpha) - \frac{3}{\alpha} P(X-\alpha) \right. \\
&\quad \left. + \frac{1}{\alpha^2} \int_0^\infty d\eta P(\eta+X-\alpha) \left\{ \lambda e^{-\lambda\eta/\alpha} \right. \right. \\
&\quad \left. \left. + \omega e^{-\omega\eta/\alpha} + \bar{\omega} e^{-\bar{\omega}\eta/\alpha} \right\} \right] \tag{27}
\end{aligned}$$

$$\begin{aligned}
F(X) &= \frac{3\theta(X-\alpha)}{4\pi\alpha^3} \left[-P'(X-\alpha) - \frac{3P(X-\alpha)}{\alpha} \right. \\
&\quad \left. + \frac{1}{\alpha^2} \int_0^\infty d\eta P(\eta+X-\alpha) \left\{ \lambda e^{(-\lambda\eta/\alpha)} + \omega e^{(-\omega\eta/\alpha)} + \bar{\omega} e^{(-\omega\eta/\alpha)} \right\} \right] \tag{28}
\end{aligned}$$

where λ , ω and $\bar{\omega}$ are the solutions of the equation

$$x^3 - 3x^2 + 6x - 6 = 0 \tag{29}$$

In terms of the variable z Eq. (28) looks like

$$\begin{aligned}
F(z) &= \frac{3\theta(z-\alpha)R(t_i)^4}{4\pi\alpha^3 v^4 t_c^4} \left[-P'(X-\alpha) - \frac{3P(X-\alpha)}{\alpha} \right. \\
&\quad \left. + \frac{1}{\alpha^2} \int_0^\infty d\eta P(\eta+X-\alpha) \left\{ \lambda e^{(-\lambda\eta/\alpha)} + \omega e^{(-\omega\eta/\alpha)} + \bar{\omega} e^{(-\omega\eta/\alpha)} \right\} \right] \\
&= \frac{R(t_i)^4}{v^4 t_c^4} f(z) \tag{30}
\end{aligned}$$

with

$$\alpha \rightarrow \frac{\alpha v t_c}{R(t_i)}; \quad \eta \rightarrow \frac{\eta v t_c}{R(t_i)} \tag{31}$$

References

- [1] See for example, Proc. QM'96, Nucl. Phys. **A 610** (1996); Proc. QM'97, Nucl. Phys. **A 638** (1998).

- [2] Proc. Lattice'96, Nucl. Phys. (proc. suppl.) **B 53** (1997).
- [3] E. Witten, Phys. Rev. **D30**, 272 (1984).
- [4] M. Crawford and D. N. Schramm, Nature **298**, 538 (1982).
- [5] L. Van Hove, TH.3623-CERN, 1983.
- [6] D. N. Schramm, at 3rd Int. Conf. Phys. & Astrophys. of Quark Gluon Plasma, March 1997, Jaipur, India, Proc. in press.
- [7] E. Aubourg et al., Nature **365** 623 (1993).
- [8] C. Alcock et al., Nature **365** 621 (1993).
- [9] J. Yang, M. S. Turner, G. Steigman, D. N. Schramm, and K. A. Olive, 1984, Ap. J. **281**, 493 (1984).
- [10] R. Schaeffer, P. Delbourgo-Salvador and J. Audouze, Nature **317**, 407 (1985).
- [11] N. C. Rana, B. Datta, S. Raha, and B. Sinha, 1990, Phys. Lett. **B240**, 175 (1990).
- [12] J. Madsen, and K. Riisager, Phys. Lett. **B 158**, 208 (1985).
- [13] C. Alcock and E. Farhi, Phys. Rev. **D32**, 1273 (1985).
- [14] J. Madsen, H. Heiselberg and K. Riisager, Phys. Rev. **D34**, 2974 (1986).
- [15] C. Alcock and A. Olinto, Phys. Rev. **D39**, 1233 (1989).
- [16] J. Madsen and M. L. Olesen, Phys. Rev. **D43**, 1069 (1991).
- [17] P. Bhattacharjee, J. Alam, B. Sinha and S. Raha, Phys. Rev. **D48**, 4630 (1993).
- [18] K. Sumiyoshi and T. Kajino, Nucl. Phys. **24**, 80 (1991).
- [19] H. Kodama, M. Sasaki, K. Sato, Prog. Theo. Phys. **68**, 1979 (1982).
- [20] G. M. Fuller, G. J. Mathews and C. R. Alcock; Phys. Rev. **D37**, 1380 (1988).
- [21] K. Iso, H. Kodama and K. Sato, Phys. Lett. **B169**, 337 (1986).

- [22] D. Stauffer, Phys. Rep. **54**, 1 (1979).
- [23] W. N. Cottingham, D. Kalafatis and R. Vinh Mau, Phys. Rev. Lett. **73**, 1328 (1994).
- [24] L. P. Csernai and J. I. Kapusta, Phys. Rev. Lett. **69**, 737 (1992).
- [25] L. D. Landau and E. M. Lifshitz, Statistical Physics (Pergamon Press, New York, 1969).
- [26] A. Heckler and C. J. Hogan, Phys. Rev. **D47**, 4256(1993).
- [27] K. Jedamzik and G. M. Fuller, Ap. J. **423**, 33 (1994) and references therein.
- [28] K. Jedamzik, G. M. Fuller and G. J. Mathews, Ap. J. **423**, 50 (1994) and references therein.
- [29] J. Alam, at Workshop on Quark Gluon Plasma and Phase Transitions in the Early Universe, Dec.'95, Puri, India.
- [30] R. Brandenberger, A. Davis and M. J. Rees, Phys. Lett. **B349**, 329 (1995).

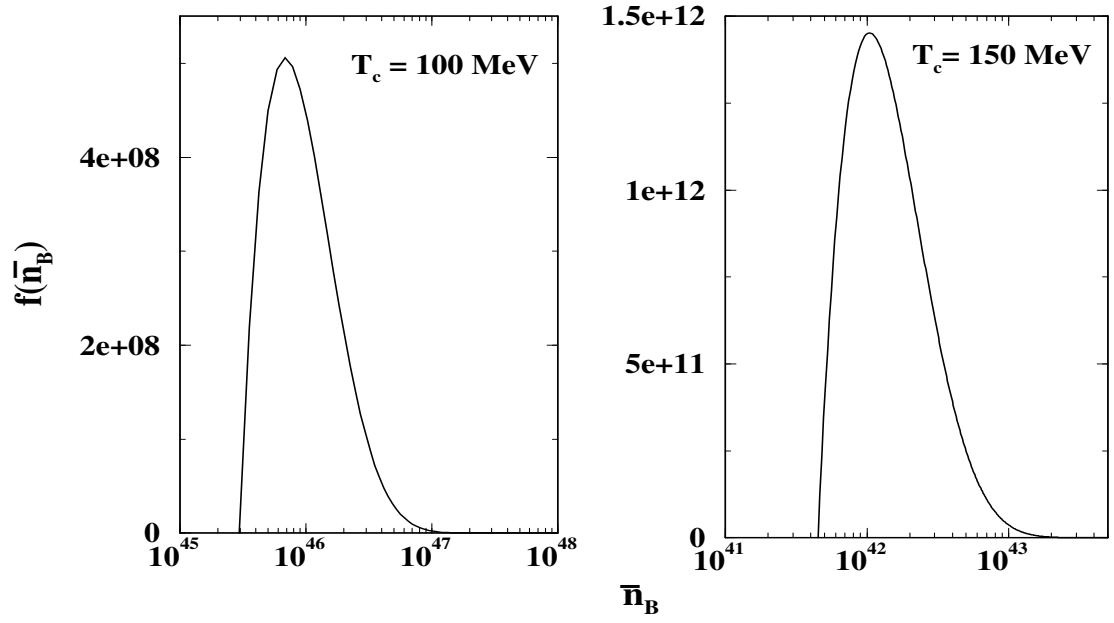


Figure 1: Distribution of QN, $f(\bar{n}_B)$, as a function of \bar{n}_B using nucleation rate proposed by Cottingham *et. al.*

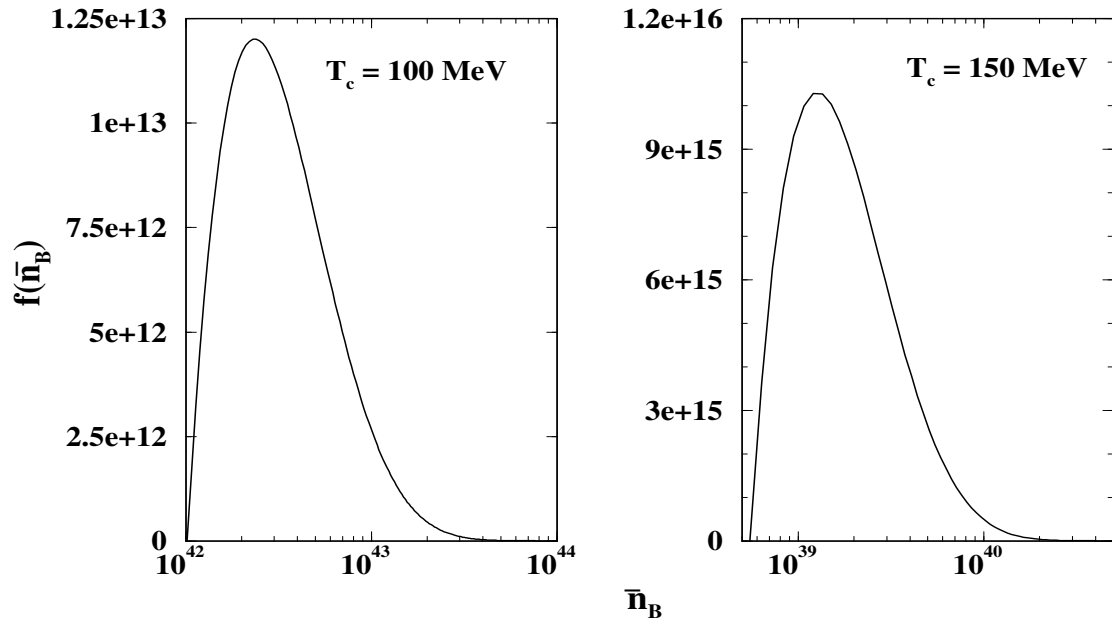


Figure 2: Same as fig. 1, using nucleation rate proposed by Csernai and Kapusta. The value of σ is 10 MeV fm^{-2} .

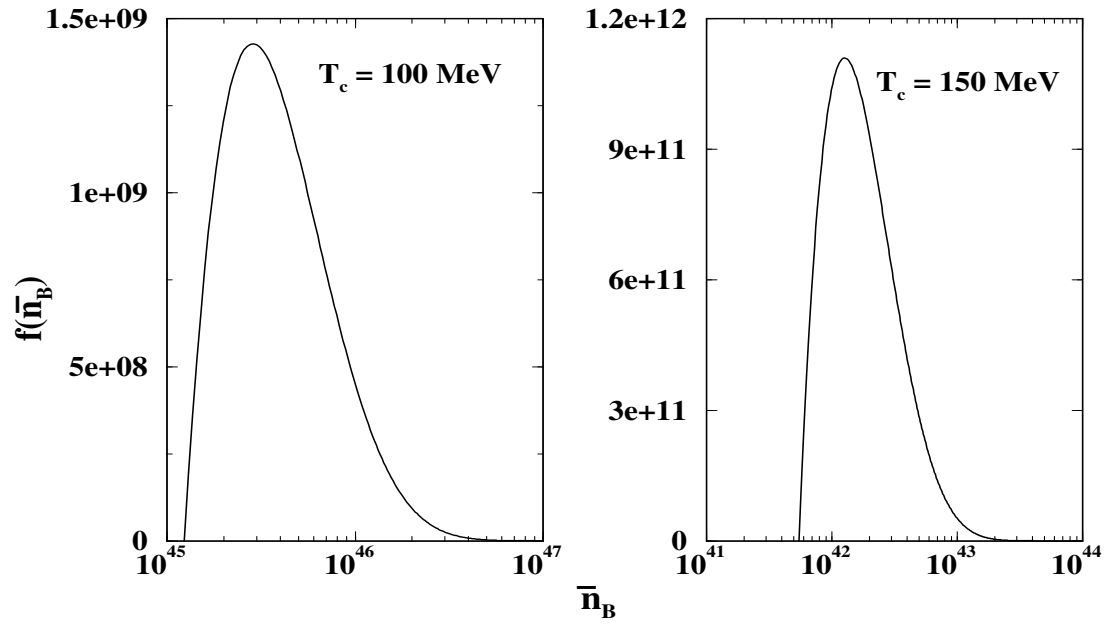


Figure 3: Same as fig. 2 with $\sigma = 50 \text{ MeV fm}^{-2}$.

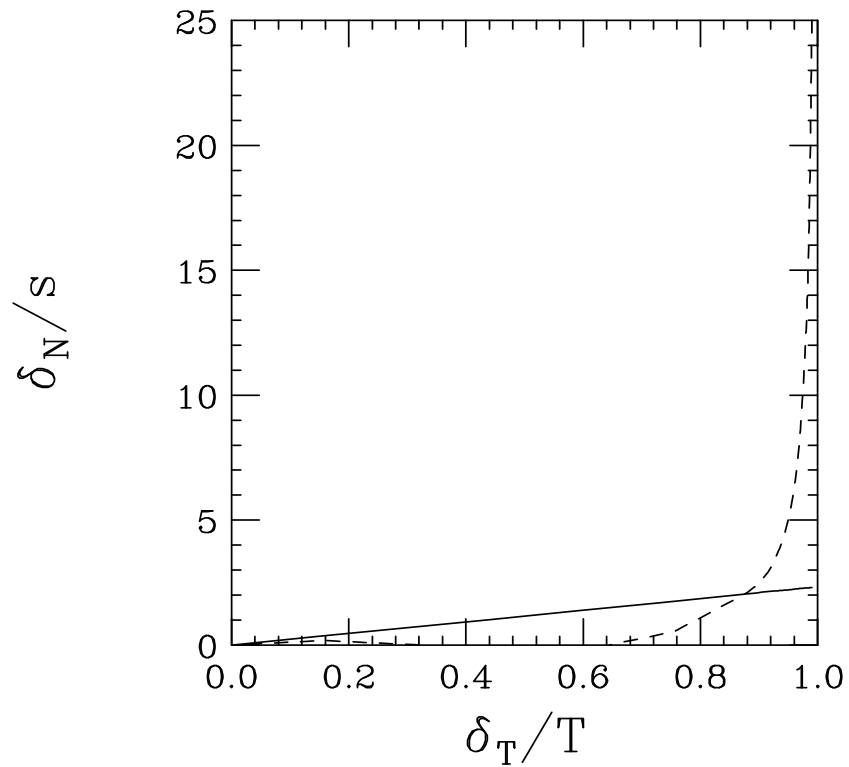


Figure 4: The relation between baryon inhomogeneity and temperature difference. The dotted line corresponds to the solution of eq. (18) and the solid line corresponds to the linear approximation as discussed in the text.

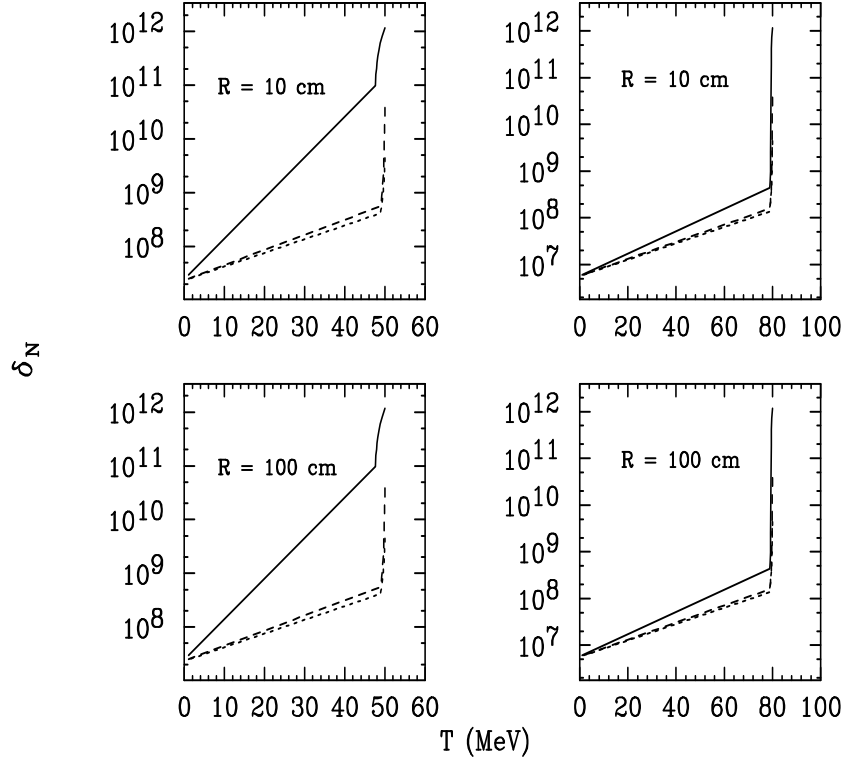


Figure 5: The evolution of baryon inhomogeneity with temperature, for different sizes of the clump and different initial temperature, due to neutrino inflation.